# Structure, tribological behaviour and photocatalytic activity of ARC-PVD $TiO_2$ coatings obtained with a modified curvilinear magnetic filter

**A.V. Taran,[1,*] I.E. Garkusha,[1] V.S. Taran,[1] A.I. Timoshenko,[1] I.A. Misiruk,[1] M.A. Sergiets,[1] T.S. Skoblo,[2] S.P. Romaniuk,[2] T.V. Maltsev,[2] V.V. Starikov,[3,*] A.A. Baturin[3] and A.G. Mamalis[4]**

[1] *National Science Centre "Kharkov Institute of Physics and Technology" (NSC KIPT), Institute of Plasma Physics, Kharkov, Ukraine*
[2] *National Technical University of Agriculture, Kharkov, Ukraine*
[3] *National Technical University "Kharkov Polytechnic Institute", Kharkov, Ukraine*
[4] *Project Centre for Nanotechnology and Advanced Engineering, NCSR "Demokritos", Athens, Greece*

$TiO_2$ coatings on AISI 430 stainless steel were produced by the vacuum-arc deposition technique with the application of a modified curvilinear magnetic filter, which allowed enhanced deposition rates up to 50 μm/h with a decrease of the quantity of macroparticles. The structure and chemical and phase compositions of the coatings were investigated by SEM together with EDX, XRF and XRD analysis. According to X-ray diffraction, the formation of single-phase $TiO_2$ took place. Mechanical and tribological properties were determined. The average hardness of the coatings was 13.8 GPa and the Young's modulus was 211 GPa. Dry friction wear tests revealed high resistance of the coating to wear and a low friction coefficient under a load of 50 N. There was a significant decrease of *E. coli* colonies during 20 min UV exposure on samples with the coating, demonstrating photocatalytic bactericidal activity.

**Keywords:** chemical composition, coating, mechanical properties, morphology, photocatalytic activity, structure, $TiO_2$

* Corresponding authors. E-mail addresses: vadym_starikov@ukr.net; avtaran@ukr.net



doi: 10.4024/N06TA19A.ntp.15.02

## 1. INTRODUCTION

Titanium dioxide ($TiO_2$) has many potential applications, such as: nontoxic coatings with high wear protection for medicine; films with high photocatalytic activity; and coatings with marked self-cleaning ability.[1]

Titanium dioxide is a well-known photocatalyst in the presence of UV light. A significant number of articles have been published on the effect of photocatalytic $TiO_2$ nanoparticles on microorganisms.[2,3] According to the literature, $TiO_2$ on stainless steel reduces the bacterial activity of *E. coli* by 99% or more, hence providing an effective antimicrobial surface coating for medical implements, thereby reducing the risk of hospital-acquired infections.[4] The efficiency of photocatalytic disinfection is attributed to oxidative damage mainly induced by reactive oxygen species (ROS) such as $O_2^-$, $H_2O_2$ and $HO^-$. They are produced by redox reactions between adsorbed species such as water and oxygen and the electrons and holes photogenerated by illumination of $TiO_2$.

$TiO_2$ films have been prepared by various methods, such as chemical vapour deposition, pulsed laser deposition, sol–gel deposition, spray pyrolysis, plasma-enhanced chemical vapour deposition, and DC/RF magnetron sputtering.[5–9]

It is well known that the method of vacuum-arc deposition is able to provide a wide range of microstructure and hardness of coatings by modulating the grain size, crystallographic orientation, lattice defect type and density, texture, as well as surface morphology and phase composition.[10–14]

---

[1] N. Berger-Keller, G. Bertrand, C. Filiatre, C. Meunier and C. Coddet, Microstructure of plasma-sprayed titania coatings deposited from spray-dried powder. *J. Surf. Coat. Technol.* **168** (2003) 281–290.

[2] M. Anpo and M. Takeuchi, The design and development of highly reactive titanium dioxide photocatalyst operating under visible light irradiation. *J. Catal.* **216** (2003) 505–516.

[3] N.R. Mathews, E.R. Morales, M.A. Cortes-Jacome and J.A.T. Antonio, $TiO_2$ thin films–Influence of annealing temperature on structural, optical and photocatalytic properties. *Solar Energy* **83** (2009) 1499–1508.

[4] C.J. Chung, H.I. Lin, H.K. Tsou, Z.Y. Shi and J.L. He, An antimicrobial $TiO_2$ coating for reducing hospital-acquired infection. *J. Biomed. Mater. Res.* **B85** (2008) 220–224.

[5] N. Martin, C. Rousselot, D. Rondot, F. Palmino and R. Mercier, Microstructure modification of amorphous titanium oxide thin films during annealing treatment. *Thin Solid Films* **300** (1997) 113–121.

[6] M. Takeuchi, N. Yamasaki and K. Tsujimaru, Preparation of $TiO_2$ thin film photocatalist on polycarbonate substrates by RF-sputtered magnetron deposition method. *Chem. Lett.* **35** (2006) 904–905.

[7] A. Verma, A.G. Joshi, A.K.Bakshi, S.M. Shivaprasad and S.A. Agnihotry, Variations in the structural, optical and electrochemical properties of $CeO_2$-$TiO_2$ films as a function of $TiO_2$ content. *Appl. Surf. Sci.* **252** (2006) 5131–5142.

[8] I. Turkevych, Y. Pihosh, M. Goto, A. Kasahara, M. Tosa, S. Kato, K. Takehana, T. Takamasu, G. Kido and N. Koguchi, Photocatalytic properties of titanium dioxide sputtered on a nanostructured substrate. *Thin Solid Films* **516** (2007) 2387–2391.

[9] M. Vishwas, S.K. Sharma, K. Narshimha Reao, S. Mohan, K.V.A. Gowda and R.P.S. Chakradhar, Influence of surfactant and annealing temperature on optical properties of sol-gel derived nano-crystalline $TiO_2$ thin films. *Spectrochim. Acta* **A75** (2010) 1073–1077.

[10] T.S. Skoblo, S.P. Romaniuk, A.I. Sidashenko, I.E. Garkusha and A.V. Taran, Strengthening method for thin-walled knives with multi-layer nanocoatings and quality assessment by non-destructive method. *J. Adv. Microsc. Res.* **13** (2018) 333–338.

[11] A.V. Taran, I.E. Garkusha and V.S. Taran, Structure of biocompatible nanocoatings obtained by physical vapour deposition on flexible polyurethane for medical applications. *J. Adv. Microsc. Res.* **13** (2018) 313–319.

The factors that limit applications of PVD coatings as complete barriers to corrosion are the presence of coating defects such as pinholes, voids, cracks and macroparticles.

In the present paper a new source of filtered vacuum arc plasma is described, which provides transportation to the condensation surface of at least 60% of the ion current emitted by cathode spots; this is 1.5 times higher than the ion current of known analogues. The deposition rate reached several tens of micrometres per hour, comparable to traditional sources of unfiltered plasma. The area occupied by macroparticles was less than 0.2% of the total coating area per 1 μm of its thickness.

In this research $TiO_2$ coatings were deposited onto AISI 430 SS surfaces using the vacuum-arc evaporation method with a modified curvilinear filter. The structure and chemical and phase compositions of the obtained coatings were investigated as well as the mechanical and tribological attributes. The photocatalytic activity of the $TiO_2$ coatings during UV exposure was measured.

## 2. EXPERIMENTAL PROCEDURES

Polished stainless steel samples of 25×25×3 mm size were used as the substrate material (roughness $R_a \approx$ H•0.09 μm). The chemical composition of the substrate was monitored by a portable XRF analyser (Z-300 LIBS, SciAps Corp., USA) and is presented in Fig.1.

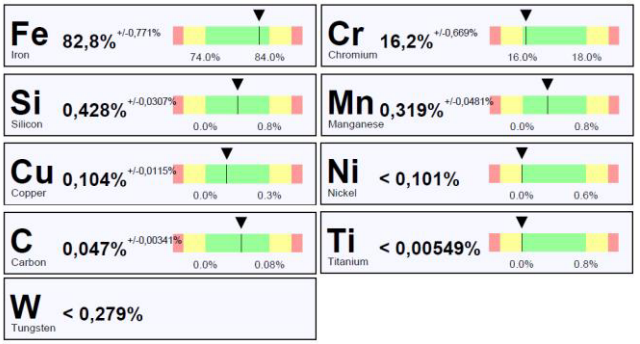


Figure 1. Chemical composition of the AISI 430 stainless steel substrates.

$TiO_x$ coatings were synthesized using vacuum-arc deposition in a Bulat-6 device. The scheme of the equipment is shown in Fig. 2. To apply coatings, the chamber was evacuated to a pressure of $1 \times 10^{-4}$ Torr. Then, a pulsed negative bias of 1000 V with a frequency of 50 kHz was applied to the sample holder. The vacuum arc was ignited ($I_d$ = 105 A) and the samples were cleaned by titanium ions in the pulsed mode for 1.5 min. Next, the chamber was filled with

[12] V. Tereshin, A. Bandura, O. Byrka, V. Chebotarev, I. Garkusha, O. Shvets and V. Taran, Coating deposition and surface modification under combined plasma processing. *Vacuum* **73** (2004) 555–559.
[13] V.V. Gasilin, Yu.N. Nezovibat'ko, G.S. Poklipach, O.M. Svets, G.S. Taran, V.I. Tereshin and A.I. Timoshenko, Filtered arc plasma discharge for coatings deposition under HF biasing of samples. *J. Appl. Plasma Science* **13** (2005) 87–93.
[14] T.S. Skoblo, S.P. Romaniuk, A.I. Sidashenko, I.E. Garkusha, V.S. Taran, A.V. Taran and R.M. Muratov, Surface morphology and mechanical properties of vacuum-arc evaporated CrN and TiN coatings on cutting tool. *J. Adv. Microsc. Res.* **13** (2018) 477–481.

oxygen to a pressure of $4 \times 10^{-3}$ Torr and titanium dioxide was deposited during 10 min at a rate of 50 μm/h. The final thickness of the $TiO_2$ coating was 5 μm.

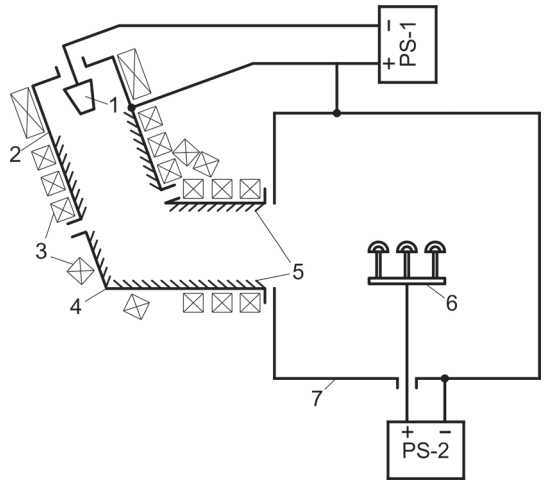


Figure 2. Scheme of the experimental deposition (coating) equipment: 1, cathode; 2, anode; 3, electromagnetic coils; 4, duct; 5, baffles; 6, samples; 7, vacuum chamber; PS-1, arc discharge power supply unit; PS-2, source of pulsed negative bias.

The surface topography of the coatings was studied using a JEOL JSM-6390LV scanning electron microscope (SEM) with an accelerating voltage of 20 kV; chemical composition was examined using EDX analysis.

X-ray diffraction (XRD) was carried out using a DRON-3M device, under Cu–Kα radiation, monochromated by (002) HOPG in a diffracted beam. The XRD line scans were done in the θ–2θ scanning mode where the incident angle θ and diffracted angle 2θ are scanned simultaneously. Crystallite size was determined from the broadenings of the corresponding X-ray spectrum peaks using Scherrer's formula.

The nanohardness was measured by a nanoindenter (G200, USA). Loading and unloading rates were 10 mN/min. Samples were tested with 7 indentations to a depth of 500 nm. The distance between indentations was 15 μm.

Tribological properties of the coating were investigated using the ball-on-disk method with an SMT-1 friction machine. The rotation frequency of the rollers (counterbody of a coated sample) was 500 $min^{-1}$. Sample loading was 50 N and 100 N. The duration of each stage was 5 min. Lubrication conditions were dry friction. The material of the roller was 100Cr6 steel.

To determine the photocatalytic activity, *E. coli* bacteria were placed in meat–peptone agar and incubated at 37 °C for 16 h. Samples of stainless steel with and without a $TiO_2$ coating were sterilized in Septolane disinfectant solution (1 $cm^3$ per L of water) for 1 h. Next, they were washed with distilled water, placed in sterilization bags and heated in an autoclave at 180 °C for 1 h. After that, the grown bacterial colonies were transplanted onto the samples of stainless steel with and without the $TiO_2$ coating. The two types of samples were exposed to UV irradiation (wavelength 253.4 nm) for 10 and 20 min.

## 3. RESULTS AND DISCUSSION

### 3.1 Structure and chemical composition

The chemical and phase compositions of the coating were studied by X-ray diffraction analysis and energy-dispersive X-ray spectroscopy (EDX). The XRD and EDX patterns of $TiO_2$ are shown in Fig. 3. The diffraction peaks indicate the formation of a crystallized $TiO_2$ coating with some strong Fe peaks from the substrate material. XRD analysis revealed the existence of a $TiO_2$ phase only (in accordance with JCPDF file 21-1236) with lattice parameters $a = 4.531$; $b = 5.498$; $c = 4.900$ (Fig. 3a).

No additional phases were observed. The EDX spectrum consists of the characteristic peaks of titanium and oxygen and low Cr, Fe, Si peaks from the substrate material (Fig. 3b). The chemical content was Ti = 29.54 atom% and O = 69.40 atom% (Table 1), indicating that the deposited films were stoichiometric. There was no variation in the chemical composition of the coating.

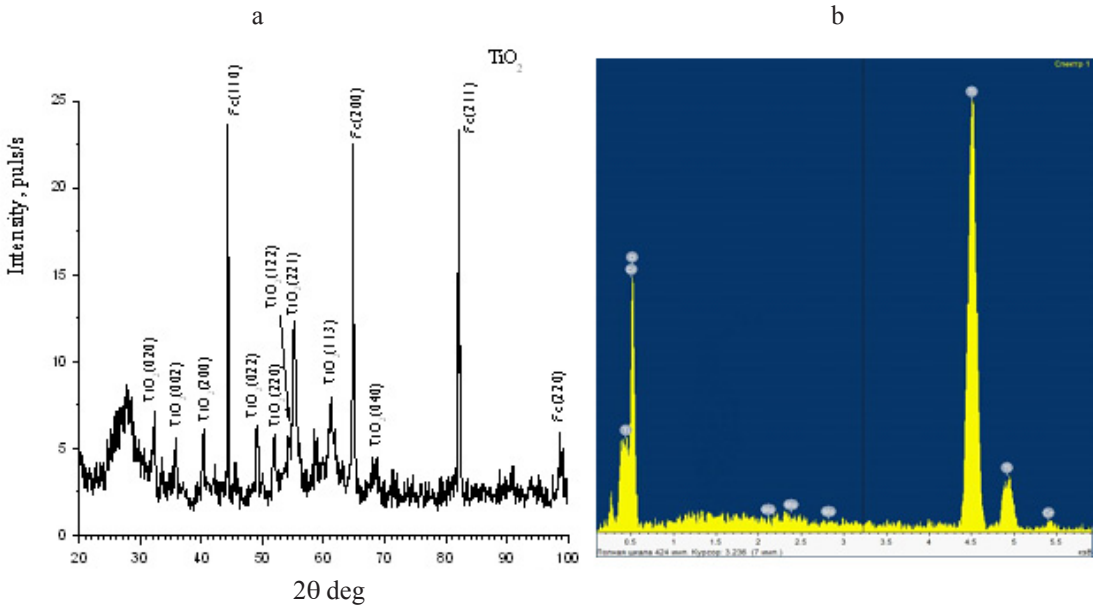


Figure 3 XRD pattern (a) and EDX spectrum (b) from a $TiO_2$ coating on AISI 430 SS.

Table 1. Chemical composition of $TiO_2$ coating in accordance with EDX.

| Element | Wt.% | Atom% |
|---|---|---|
| O | 43.00 | 69.40 |
| Ti | 54.79 | 29.54 |
| Cr | 1.40 | 0.69 |
| Fe | 0.81 | 0.37 |

The crystallite size $D$ of the deposited $TiO_2$ coatings was calculated from the full width at half maximum intensity (FWHM, β) of the X-ray diffraction angle (θ) of the peak and the wavelength (λ) of copper X-ray radiation using Debye–Scherrer's relation, taking into account that no strains were developed in the films:

$$D = K\lambda / \beta\cos\theta \quad (1)$$

where $K$ is a constant with the value of 0.9 for copper X-ray radiation and θ the diffraction angle. The crystallite size of the titanium dioxide film was found to be 21 nm.

The surface morphology of deposited $TiO_2$ coating was also investigated. Fig. 4 shows SEM images of $TiO_2$ coating at various magnifications. The quality of the coating revealed very low amounts of macroparticles distributed over the surface. The coating was constituted from relatively small spheroidal $TiO_2$ nanoparticles aggregated to form clusters. The coating is porous but free from cracks. The EDX mapping of the distribution of chemical elements (Ti, O and C) over the surface was shown in Fig. 4d.

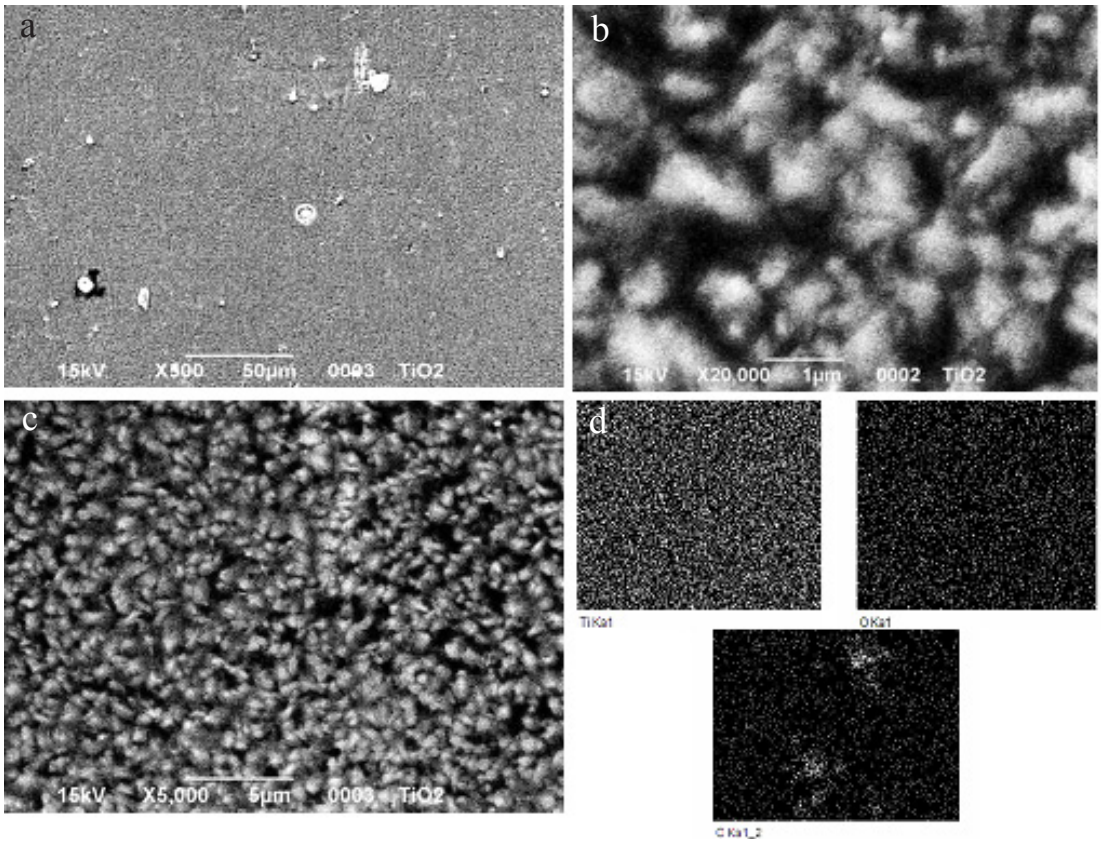


Figure 4. SEM images (a–c) and EDX mapping (d) of $TiO_2$ coated onto AISI 430.

### 3.2 Mechanical properties

The $E/H$ ratio is a criterion of the plastic index of materials, and a small ratio indicates elastic deformation during contact motion, which is beneficial for enhancing the tribological performance of the material. The $H^3/E^{*2}$ ratio (where the effective elastic modulus $E^* = E/(1-\mu^2)$, with μ being Poisson's ratio) is a qualitative comparative characteristic of the plastic deformation resistance of the material. The nanoidentation diagrams for the $TiO_2$ coating are presented in Fig. 5. The $H$ and $E$ values for 7 indentations are summarized in Table 2. According to these tests, the average nanohardness value for $TiO_2$ is 13.8 GPa with a data spread of 9.5%; the average value of the elastic modulus is 211.072 Gpa with a data spread of 7.7%.

The shear modulus ($G$) and yield stress ($\sigma_T$) are defined as $G = E / 2 \times (1 + \mu)$ and $\sigma_T = H\mu / 3$, respectively (Tables 2 and 3).

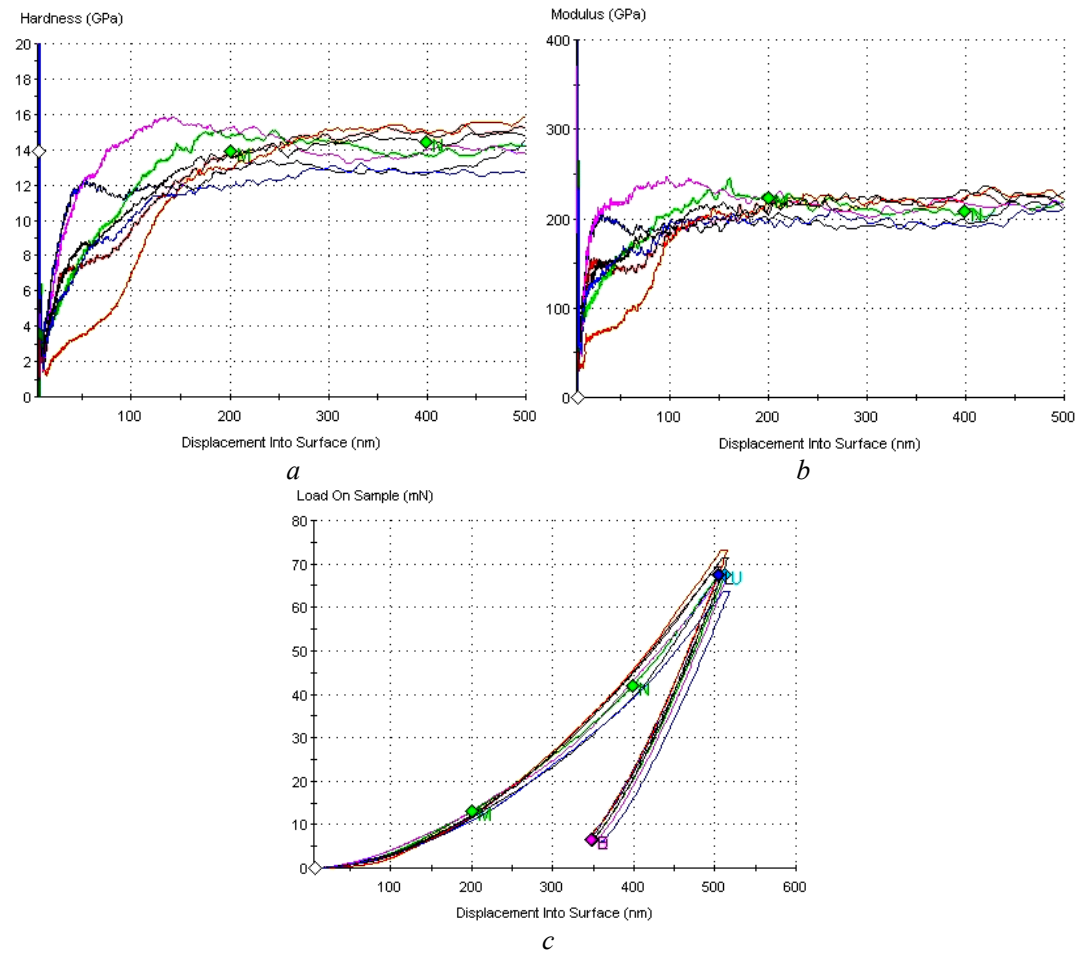


Figure 5. Nanoindentation diagrams for the $TiO_2$ coating: nanohardness (a), elastic modulus (b); loading–unloading diagram (c).

Table 2. Mechanical test results for the $TiO_2$ coating.

| Test | *E*/GPa | *H*/Gpa | *H*/*E* | $H^3/E^{*2}$ | *G*/GPa | $\sigma_T$/GPa |
|---|---|---|---|---|---|---|
| 1 | 216.814 | 14.515 | 0.067 | 0.057 | 135.51 | 4.83 |
| 2 | 194.802 | 12.956 | 0.067 | 0.050 | 121.75 | 4.31 |
| 3 | 214.05 | 14.36 | 0.067 | 0.057 | 133.78 | 4.78 |
| 4 | 220.587 | 14.447 | 0.065 | 0.054 | 137.87 | 4.81 |
| 5 | 214.036 | 14.114 | 0.066 | 0.054 | 133.77 | 4.70 |
| 6 | 219.956 | 14.214 | 0.065 | 0.052 | 137.47 | 4.73 |
| 7 | 197.258 | 12.558 | 0.064 | 0.045 | 123.29 | 4.18 |
| **Average** | **211.072** | **13.881** | **0.066** | **0.053** | **131.92** | **4.62** |

Table 3. Mechanical properties of AISI 430.

| Test | *E*/GPa | *H*/GPa | *H*/*E* | $H^3/E^{*2}$ | *G*/GPa | $\sigma_T$/GPa |
|---|---|---|---|---|---|---|
| 1 | 204.382 | 3.915 | 0.019 | 0.001 | 127.74 | 1.30 |
| 2 | 217.567 | 5.01 | 0.023 | 0.002 | 135.98 | 1.67 |
| 3 | 204.496 | 3.727 | 0.018 | 0.001 | 127.81 | 1.24 |
| 4 | 184.049 | 4.084 | 0.022 | 0.002 | 115.03 | 1.36 |
| 5 | 203.588 | 3.872 | 0.019 | 0.001 | 127.24 | 1.29 |
| 6 | 205.773 | 3.99 | 0.019 | 0.001 | 128.61 | 1.33 |
| 7 | 198.272 | 3.61 | 0.018 | 0.001 | 123.92 | 1.20 |
| **Average** | **202.590** | **4.030** | **0.020** | **0.001** | **126.62** | **1.342** |

### 3.3 Tribological behaviour

Tribological properties of the $TiO_2$ coating were investigated using friction machine SMT-1. After testing the weight wear and friction coefficient evaluation, values of the initial nanohardness and after two-stage loading were obtained (Table 4).

Table 4. Mechanical properties of the $TiO_2$ coating.

| Controlled parameter | Measurement condition | Parameter value |
|---|---|---|
| Weight wear/g | Coating | –0.0116 |
| | Roller | –0.0074 |
| Microhardness/GPa | Initially | 7.76 |
| | After testing | 6.02 |
| Friction coefficient | With a 50 N load | 0.63 |
| | With a 100 N load | 0.92 |

Considering the tougher conditions of dry friction, the test results show a high resistance of the coating to wear in combination with a low friction coefficient under a load of 50 N (Table 4). When the load is 100 N the friction coefficient increases by 43% due to wear of the coating and the formation of friction contacts with sample substrate. The nanohardness after testing decreased by 13% compared with the initial value.

### 3.4 Photocatalytic activity

The results show a significant decrease of *E. coli* colonies with increasing irradiation time for samples with the $TiO_2$ coating (Fig. 6).

| Exposure time | Sample | |
|---|---|---|
| | Without $TiO_2$ coating | With $TiO_2$ coating |
| 10 min |  |  |
| 20 min |  |  |

Figure 6. Progressive elimination of *E. coli* colonies on stainless steel substrates with and without $TiO_2$ during UV light exposure during 10 and 20 min.

#### 4. CONCLUSIONS

$TiO_2$ coatings on AISI 430 stainless steel were produced by the vacuum-arc deposition technique with the use of a modified curvilinear magnetic filter, which allowed enhanced deposition rates up to 50 μm/h and decreased the quantity of macroparticles deposited. XRD analysis of the coatings revealed the existence of a single $TiO_2$ phase with the chemical composition: Ti, 29.54 atom%; O, 69.40 atom%.

The coating was composed of relatively small globular $TiO_2$ nanoparticles aggregated to form clusters. The coating was porous but free of cracks and had very low amounts of macroparticles distributed over the surface.

The average nanohardness of the $TiO_2$ coating was 13.8 GPa and the average value of the elastic modulus was 211.701 GPa. The coating demonstrates high resistance to wear and has a low friction coefficient under a load of 50 N.

By inoculating samples of uncoated and coated stainless steel, a significant decrease of *E. coli* colonies with increasing irradiation time on $TiO_2$-coated samples was observed.